

# Construction and Commissioning of HLS Injection Bump System<sup>\*</sup>

SHANG Lei<sup>1)</sup> WANG Xiang-Qi WANG Lin JIANG Dao-Man ZHAO Feng

(National Synchrotron Radiation Laboratory,  
University of Science and Technology of China, Hefei 230029, China)

**Abstract** This paper describes the construction and the commissioning of the new injection bump system of HLS ring. An emphasis of the discussion is put on various errors of the system and the method of evaluation and reduction. After some improvements and fine adjustment, an average injection rate of 2—6mA/s was obtained in the daily operation and a maximum accumulated current of 400mA achieved. The injection system has run for almost two years and played an important role in the operation of the light source.

**Key words** injection system, kicker magnet, ceramics chamber, error, commissioning

## 1 Introduction

HLS is a second-generation, dedicated synchrotron radiation source. It consists of three major facilities which are the 200MeV Linac, the transport line and the 800MeV storage ring. In order to enhance the stability of the light source and build more beam lines to make full use of the synchrotron radiation, an upgrade project of the machine was initiated in 1998. Among many upgrades of sub-systems, the new injection bump system<sup>[1, 2]</sup> is a very important one. The old injection system employed three air-core magnets. The formation of bump orbit for injection depends largely on the parameters of lattice configuration. The correct bump orbit can not be formed in some designed lattice modes. The kicker magnets also occupied the locations, which were originally intended for installing two sextuple magnets. The air-core magnets were housed in stainless steel vacuum chambers and they make a considerable contribution to the impedance of the storage ring. In the new injection system, four window-frame ferrite kickers were used and mounted in one straight section of the stor-

age ring. The formation of bump orbit is independent of the lattice parameters. All the kicker magnets have the same deflection angles. The adjustment of parameters is simplified. Ceramic chambers with inner surface coating were developed and installed inside the ferrite yokes. Kicker and septum modulators were also rebuilt in which more advanced technology was employed<sup>[3]</sup>.

The commissioning of the injection bump can be divided by two phases. The first phase is in Sep. 2002. The accumulated current cannot surpass 20—30mA even with a subsidiary DC bump orbit, which is caused by the unsatisfactory coating of the ceramic chambers. After the improvement and reinstallation of the ceramic chambers, the second phase commissioning began in Feb. 2003 and the beam was successfully accumulated to more than 350mA and reached the design goal. Up to now, the system has run for almost two years. The ceramic chambers and their inner surface coating are reliable with no indication of deterioration. The kicker modulators run stably and need little maintenance.

Received 14 June 2005

<sup>\*</sup>Supported by the Phase II Project of NSRL

1) E-mail: lshang@ustc.edu.cn

## 2 Injection system and error analysis

### 2.1 The new injection bump system

Electron beam is transported through the transfer line to the storage ring with a  $-6^\circ$  horizontal angle. The septum magnet deflects the beam by a  $+6^\circ$  angle and makes the injected beam to be parallel to the stored beam. The four kickers bump the stored beam orbit horizontally by a maximum offset of 32mm and move the orbit close to the septum strip and bring the injected beam within the storage ring aperture as shown in Fig. 1. The accumulated beams are then be ramped to 800MeV.

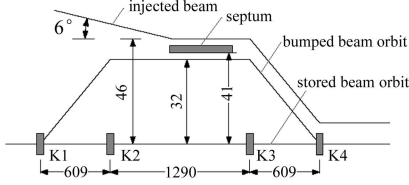


Fig. 1. New injection bump orbit.  
Units are in millimeters.

Table 1. Major parameters of the new injection system.

injection energy	200MeV
number of kickers	4
deflecting angle	52mrad
peak magnetic field	1250 Gauss
peak pulse current	3250A per magnet
physical dimensions of kicker magnets	length
	width
	286mm×140mm K1 and K2
	286mm×180mm K3 and K4
distance from K1 to K4	2.5m
maximum bump offset	32mm
magnetic field waveform	damping sine wave with a bottom width of 3.5μs
repetition rate	0.5Hz

Considering that the repetition rate is very low which is limited by the damping time and that the life time is very short, which is caused by Touschek effect corresponding to the injected electron beam of 200MeV, a multi-turn injection scheme was adopted in order to increase the accumulation rate. The analysis of multi-turn injection was presented in paper<sup>[2]</sup>.

### 2.2 Scheme of power supplies connection

In the new design, K1 and K2 magnets are identical and are powered in parallel by one modulator. K3

and K4 magnets, which are also identical but have different dimensions from K1 and K2, are powered by another modulator. The modulator employs a lumped RLC discharge topology and only one thyatron switch. The amplitude of pulsed current delivered to each magnet can be adjusted as illustrated in Fig. 2. The timing between two kickers cannot be adjusted but there is no time jitter between two adjacent kickers in such a scheme.

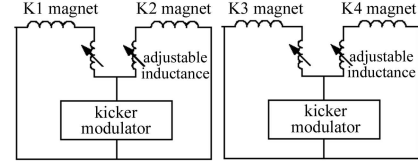


Fig. 2. The kicker modulators connection.

### 2.3 Error sources and analysis

In ideal condition, the deflection angles of the four kicker magnets satisfy:

$$\theta_1 = -\theta_2 = -\theta_3 = \theta_4, \quad (1)$$

and they generate a perfect bump orbit. There is no orbit distortion outside the bump. But in real situation, beams see different deflection angles because of the various errors. They can be categorized as follows:

- 1) Balance of current feeding to a pair of kickers which are connected in parallel.
- 2) Inhomogeneity of the longitudinal integrated B-field.
- 3) Deformation and time error of the pulsed B-field which is caused by the inner surface coating of ceramic chambers.
- 4) Installation and alignment error, etc.

Errors also can be divided into two types according to their effects, which are the deflection error and the displacement error. In Fig. 3, beam has an angular error  $\Delta x'$  after leaving the injection bump. This is caused by the non-zero value of integration field of all the four kickers along  $z$  direction.

$$\Delta x' = \frac{e}{\gamma m_0 c} \int_0^L B_y(z) dz \neq 0. \quad (2)$$

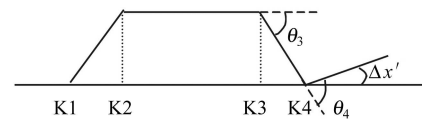


Fig. 3. Deflection error.

In Fig. 4 beam has a displacement  $\Delta x$  after leaving injection bump, which is caused by the non-zero value of the second integration of the field as shown in Fig. 4. That is:

$$\Delta x = \frac{e}{\gamma m_0 c} \int_0^L \int_0^u B_y(u) du dz \neq 0. \quad (3)$$

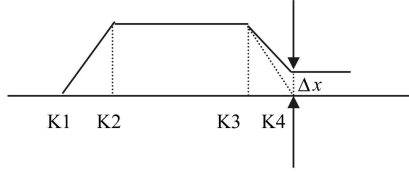


Fig. 4. Displacement error.

In real situation both errors exist. However, the deflection error is much more serious than the displacement error. Therefore, much attention should be paid to this kind of errors. In the new design, the most important thing is to make a pair of kickers, for example K1 and K2, as identical as possible in order to reduce the deflection error. From this point of view, it is a good choice to use only one modulator for a pair of kickers. Assuming there was no error between a pair of kickers K1 and K2 or K3 and K4, the error between two pairs of magnets (K1-K2 and K3-K4) has only displacement effect and small influence.

## 2.4 Summary of major error tolerances

Through the simulation study, the error tolerances can be obtained and summarized as follows<sup>[4]</sup>;

- The average time difference seen by the electron beam passing through a pair of kicker magnets (e.g. K1 and K2) must be less than  $\pm 5\text{ns}$ ;
- Homogeneity of the longitudinal integrated peak field at different horizontal offset in a magnet must be less than 0.5%.

## 3 Commissioning and improvement

From above analysis, we know that the error tolerance is very tight especially between a pair of kickers. In order to reduce errors and increase the injection rate the following measures were taken during the commissioning stage.

### 3.1 Adjustment of the balance of current

Firstly, we adjust the balance of the currents feeding to a pair of kicker magnets. A turn-by-turn BPM

was used to evaluate the orbit distortion. When the balance is not good enough, the transient orbit distortion can be clearly detected from the turn-by-turn BPM which is located near Quadrupole Q7 as seen from Fig. 5.

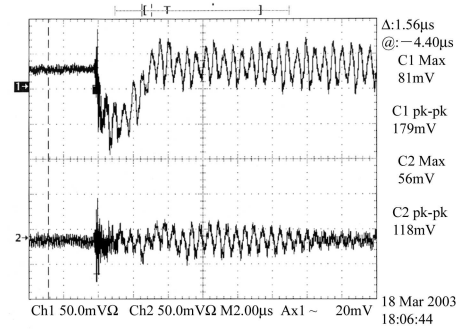


Fig. 5. BPM signals when the balance of current is not good. Upper:  $x$  direction; lower:  $y$  direction.

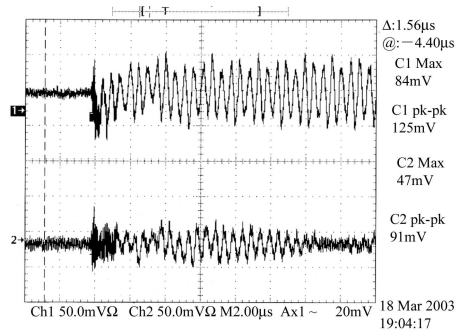


Fig. 6. BPM signal when the balance is good. Upper:  $x$  direction; lower:  $y$  direction.

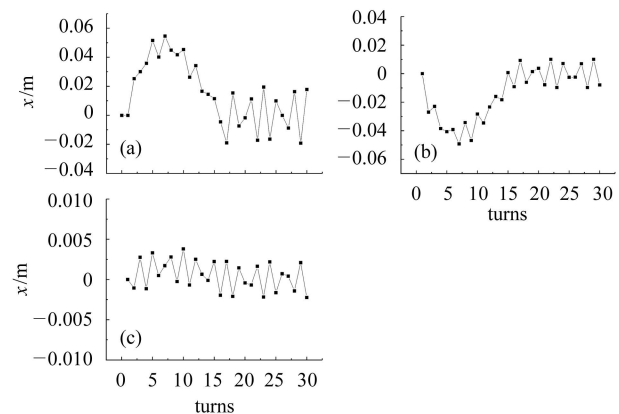


Fig. 7. Transient orbit distortion of the stored beam at Q7.

(At Q7, the horizontal  $\beta$ -function has a maximum value. The data were obtained from the tracking study in which the code Dimad was employed. The input conditions are; (a)  $K3 < K4$ , 10% (b)  $K3 > K4$ , 10%, (c)  $K3 = K4$ ).

When a better balance is reached, the oscillation signal is like Fig. 6. An over adjustment produces an opposite distortion in  $x$  direction. The correctness of the method can be confirmed by the simulation study which is shown in Fig. 7.

### 3.2 Improvement of coating<sup>[5]</sup>

The coating film of the ceramic chamber induces an eddy current effect and generates a time error. The first ceramic chamber coated by the method of Fix-Quantity Deposition is not satisfactory. The rise time difference between a pair of kickers is as high as 100ns. It was the major error source. We develop a two-coil pulsed magnetic field measurement system to examine the defective pipes. After improvement the error is reduced to only  $\pm 4$ ns. The injection rate was improved greatly and the problem was solved successfully.

### 3.3 DC auxiliary bump

DC auxiliary bump is proved to be an effective method to reduce errors of the pulsed filed. In GPLS mode a DC bump can be generated by four corrector

magnets as shown in Fig. 8.

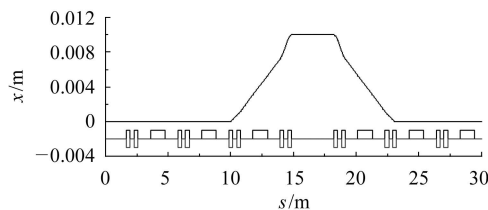


Fig. 8. A 10mm DC bump generated by Q4N, Q1N, Q1E, Q4E with deflection angles of 1.4mrad, 0.5mrad, 0.5mrad and 1.4mrad respectively.

By experience, a 5—7mm DC bump plus a 25—27mm pulsed bump have a very good injection performance. They are adopted as routine operation parameters.

*The author would like to thank the helpful discussion, advice, and support of Prof. D. H. He, Prof. Y. J. Pei, Prof. Z. P. Liu, Prof. W. M. Li and Prof. J. H. Wang in the upgrade project of the HLS injection system. We are also grateful to Mr. Y. Peng, Mr. T. Wu, Mr. Y. Z. Liu and Ms. X. Jiang for their work in improving the coating of the ceramic chambers.*

## References

- LIU Zu-Ping, LI Wei-Min. Progress of the NSRL Phase Two Project. In: Proceedings of the Second Asian Particle Accelerator Conference. Beijing, China, 2001. 235—238
- SHANG Lei, WANG Xiang-Qi, PEI Yuan-Ji. Nucl. Instrum. Methods in Phys. Res., 1998, **406**(2): 171—181
- SHANG Lei et al. New Injection Kicker Modulators for HLS Ring. IEEE, Proceedings of PAC2001, **5**: 4059—4061
- SHANG Lei. Physical Design of HLS New Injection Bump System and R&D of Ceramic Chambers. Ph.D. Thesis, USTC, Dec. 1999, (in Chinese)  
(尚雷. HLS新注入系统物理设计及陶瓷真空室的研制. 中国科学技术大学博士论文, 1999, 12)
- SHANG Lei, WANG Xiang-Qi, JIANG Dao-Man et al. IEEE Transaction on Nuclear Science, 2004, **51**(1): 2454—2459

## 合肥光源注入系统建造与调试\*

尚雷<sup>1)</sup> 王相蓁 王琳 蒋道满 赵枫

(中国科学技术大学国家同步辐射实验室 合肥 230029)

**摘要** 介绍了HLS(合肥光源)储存环注入系统建造与调试情况. 重点讨论了各种公差、公差判断及抑制措施, 经过改进与及仔细调整, 得到了平均累积速率2—6mA/s的日常运行水平, 最高累积流强400mA, 该系统已经稳定使用近两年, 在光源的运行中起到了重要作用.

**关键词** 注入系统 冲击磁铁 陶瓷真空室 公差 调试

2005 - 06 - 14 收稿

\*国家计委重大科学工程“国家同步辐射实验室二期工程”项目资助

1) E-mail: lshang@ustc.edu.cn